Available online at www.sciencedirect.com

ScienceDirect

Procedia IUTAM 22 (2017) 237 – 243

Procedia IUTAM

www.elsevier.com/locate/procedia

IUTAM Symposium on Nonlinear and Delayed Dynamics of Mechatronic Systems

Experimental investigation of the vibro-impact capsule system

Yang Liu[a,*], Haibo Jiang[b], Ekaterina Pavlovskaia[c], Marian Wiercigroch[c]

[a]*College of Engineering Mathematics and Physical Sciences, University of Exeter, Rennes Drive, Exeter EX4 4RN, UK*
[b]*School of Mathematics and Statistics, Yancheng Teachers University, Yancheng 224002, China*
[c]*Centre for Applied Dynamics Research, School of Engineering, University of Aberdeen, Aberdeen AB24 3UE, UK*

Abstract

This paper presents an experimental investigation of the vibro-impact capsule system, which has potential applications in capsule endoscopy and engineering pipeline inspection. The experimental results obtained using novel test rig are used to verify the modelling approach where non-smooth multibody dynamics is applied to describe the motion of the system, and comparisons between numerical simulations and experiments are given. After an appropriate re-scaling, the findings of this work could provide a better insight into the behaviour of such systems which are subject to harmonic excitation.

Peer-review under responsibility of organizing committee of the IUTAM Symposium on Nonlinear and Delayed Dynamics of Mechatronic Systems

Keywords: Capsule system; non-smooth dynamical system; vibro-impact; friction; experiment.

1. Introduction

Developing small-size robots with accessibility of the complex environment, such as pipeline [1,2,3] and gastrointestinal tract [4,5,6,7] for diagnosis, has been a challenge task over the past decade, particularly in the design of the external driving mechanisms (e.g. leg) for locomotion [8]. The complicated design of such tools and difficulties in their control are the bottlenecks that restrict their development in microsize. Alternatively, the self-propulsion robots driven by autogenous internal interactive forces is a promising solution with growing interests in recent years [9,10,11,12,13]. The driving principle of these systems originally proposed by Chernousko [14] is that the rectilinear motion of a system can be obtained through overcoming external resistance described as dry friction force using a periodically driven internal mass interacting with the main body of the system (see Fig. 1(a,b)). The advantage of this method is that no external driving mechanism is required, so the system can be encapsulated and move independently in the complex environment [16]. This paper presents an experimental study for this type of capsule system by using a newly designed test bed which allows one to investigate the influence of control parameters, such as impact stiffness, excitation frequency and amplitude, on system dynamics. The findings in this paper have significance in prototype design and fabrication which could be scaled up/down for the systems in any size.

*Corresponding author. Tel.: +44-1392-724654.
E-mail address: y.liu2@exeter.ac.uk

Peer-review under responsibility of organizing committee of the IUTAM Symposium on Nonlinear and Delayed Dynamics of Mechatronic Systems
doi:10.1016/j.piutam.2017.08.029

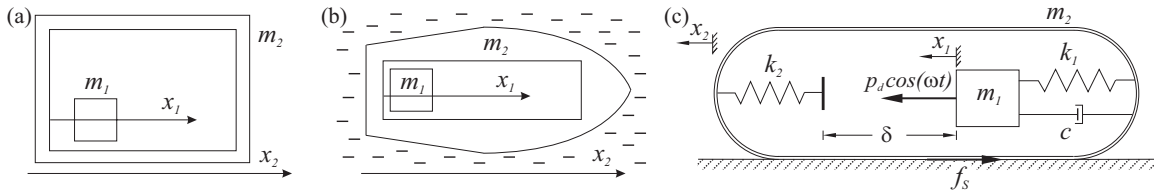

Fig. 1. Physical models of the capsule system: (a) on a resistive surface; (b) in a resistive medium [15]; (c) the vibro-impact capsule system

In the recent years, vibro-impact driven robots have attracted great attention from the robotics community. Nagy *et al.* [9] studied the motion of a complex micro-robot exhibiting impacts and friction numerically and experimentally. They have found that the stiction and sliding of the robot are governed by excitation frequency and friction, while impact around the resonant frequency of the oscillator does not contribute to robot's propulsion. In this paper, we will also consider both non-smooth nonlinearities (i.e. friction and impact) numerically and experimentally, and further investigate the dynamical responses of this type of robot under variations of different control parameters. One of the notable differences between the micro-robot [9] and the capsule system studied in this paper is that, the former is operated in the kilohertz range of oscillation and direct observation of the non-smooth phenomena at the micro-scale is impossible, while the later is controlled at a much lower frequency so that vibro-impact responses of the system can be easily observed. Hence after an appropriate re-scaling, the findings of this paper could provide a better insight for these micro-sized robots subject to high frequency excitation, and the novel experimental test bed can be used to predict the dynamical behaviour of these robots.

A major obstacle of current miniature capsule robots is the limited amount of power which restrains its operational duration. A multi-coil inductive powering system [10] was designed for a vibratory driven capsule robot to address the power shortage issue in capsule endoscope, and a frictional reduction approach of this robot using a rotational vibratory motor was studied [11]. Since only partial power contributes to the rectilinear motion of the robot, rotational vibration is not considered as an efficient way of driving. A capsule robot driven by a linear vibratory actuator was designed [17], and its friction resistance in gastrointestinal tract was modelled [18]. In order to enhance the rectilinear progression of the capsule robot, we introduce a stop for the linear vibratory actuator which could produce notable impacts for the system. The dynamics of such a vibro-impact capsule system was studied numerically, and it has found that the control parameters for the best progression and for the minimum energy consumption are different, and therefore, a trade-off between the best progression and the energy consumption is required in order to optimize the capsule motion [12]. A preliminary experimental study was carried out [19], and an experimental verification of the vibro-impact capsule model was presented which showed a good agreement in a broad range of control parameters [20]. The conducted bifurcation analysis indicated that the behaviour of the system was mainly periodic and that a fine tuning of the control parameters can significantly improve system performance. In this paper, we focus on the comparison of numerical and experimental results, and elucidate the discrepancies encountered by Liu *et al.* [20].

2. Mathematical Modelling

The vibro-impact capsule system is modelled as a two degree-of-freedom dynamical system depicted in Fig. 1(c), where a movable internal mass m_1 is driven by a harmonic force with amplitude p_d and frequency ω generated by a linear actuator. The actuator contains a movable part connected to the internal mass and a fixed part mounted on the rigid capsule m_2. We simplify the model of the actuator here and represent the interaction between the internal mass and the capsule by using a linear spring with stiffness k_1 and a viscous damper with damping coefficient c. x_1 and x_2 represent the absolute displacements of the internal mass and the capsule, respectively. The internal mass contacts a weightless plate connected to the capsule by a secondary linear spring with stiffness k_2 when the relative displacement x_1-x_2 is larger or equals to the gap δ. When the force acting on the capsule exceeds the threshold of the dry friction force f_s between the capsule and the supporting environmental surface, bidirectional motion of the capsule will occur, and the dynamic friction force f_d will be applied to the capsule. The comprehensive equations of motion for the

vibro-impact capsule system can be written as

$$\begin{aligned}
\dot{x}_1 &= y_1,\\
\dot{y}_1 &= [p_d\cos(\omega t) + k_1(x_2 - x_1) + c(y_2 - y_1) - h_1k_2(x_1 - x_2 - \delta)]/m_1,\\
\dot{x}_2 &= y_2[h_2(1 - h_1) + h_3h_1],\\
\dot{y}_2 &= [h_2(1 - h_1) + h_3h_1][-f_d - k_1(x_2 - x_1) - c(y_2 - y_1) + h_1k_2(x_1 - x_2 - \delta)]/m_2,
\end{aligned} \tag{1}$$

where f_d is given by the Coulomb Stribeck model[16], $f_d = \mu_d(1+e^{-|\dot{x}_2|/v_s})(m_1+m_2)g\cdot\mathrm{sign}(\dot{x}_2)$, μ_d is the dynamic friction coefficient, v_s is the Stribeck velocity, and g is the acceleration due to gravity. The switching functions h_i $(i = 1, ..3)$ are given by $h_1 = h(x_1-x_2-\delta)$, $h_2 = h(\mid k_1(x_2-x_1)+c(y_2-y_1)\mid -f_s)$, and $h_3 = h(\mid k_1(x_2-x_1)+c(y_2-y_1)-k_2(x_1-x_2-\delta)\mid -f_s)$, where $h(\cdot)$ is the Heaviside function, f_s is given as $f_s = \mu_s(m_1 + m_2)g$, and μ_s is the static friction coefficient.

3. Experimental set-up

The photograph of the test bed is shown in Fig. 2(a). It consists of a linear DC servomotor mounted on a base frame connected with a standing frame which holds a support spring with an adjustable stiffness k_2. The motor has a movable rod with the mass m_1 harmonically excited with a desired frequency ω and amplitude p_d through the electro-magnetic fields generated by the coils within the motor. Although a nonlinear resistance force keeps the rod in place when the motor is switched on, we assume that this force could be linearized around the working point which could be characterised by constant coefficients k_1 and c for the displacement and velocity, respectively. A gap δ exists between the rod and the support spring, and the rod contacts with the support spring when their relative displacement is larger or equals to the gap. The schematics of the experimental setup is shown in Fig. 2(b), where the absolute displacement of the rod is x_1, and the absolute displacement of the base frame is x_2 which is measured by a linear variable differential transformer (LVDT) displacement transducer. The relative displacement of the rod and the base frame $x_1 - x_2$ is measured via three hall sensors within the motor. The acceleration of the rod $\ddot{x}_1$ is obtained using an accelerometer mounted directly on the rod.

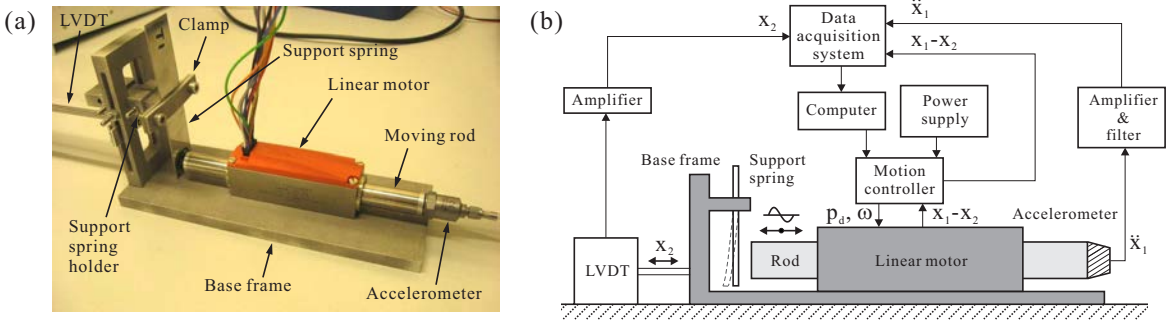

Fig. 2. (a) Photograph of the test bed and (b) schematics of the experimental setup[20]

The total weight of the rod and the accelerometer provides the mass m_1, and the weight of the rest components including the motor body, the standing and base frames, and the support spring gives the mass m_2. Both masses were simply measured by weighting each element and kept constant throughout the experiment. To determine the values of the coefficients k_1 and c, free vibration test was carried out by keeping the motor switched on and stationary, displacing the rod from its equilibrium position and recording the displacement of the oscillating rod. The frequency of the obtained vibrations, ω_o allows to work out the coefficient k_1 with known m_1 and the coefficient c was found using the logarithmic decrement method. The stiffness of the support spring, k_2 was determined through static tests, and it can be varied by changing the length of the support spring. The current of the motor was measured via motion controller so that the forcing amplitude, p_d can be determined in real-time. The linear relationship between the current of the motor and the force applying to the rod is presented in Fig. 3(a). The gap between the rod and the support spring, δ can be adjusted by setting the initial absolute position of the rod.

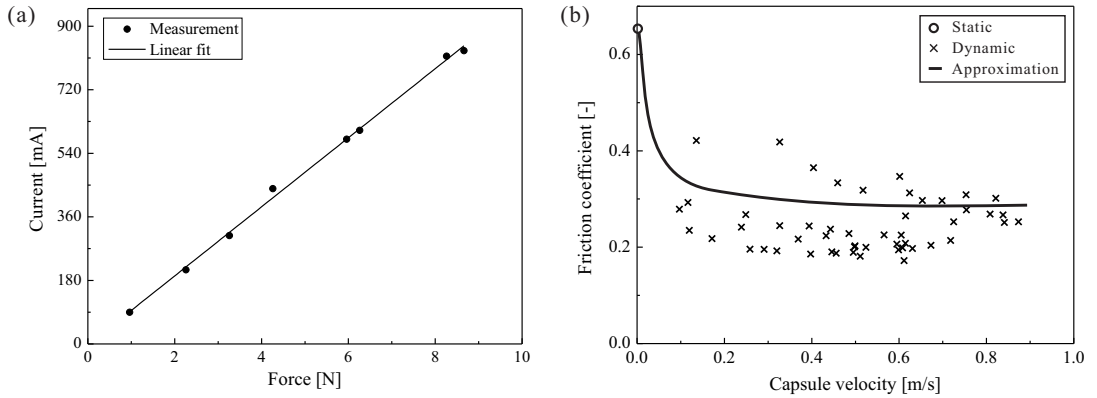

Fig. 3. (a) Motor current as a function of the resistent force on the rod and (b) identified friction coefficients as a function of capsule velocity[20].

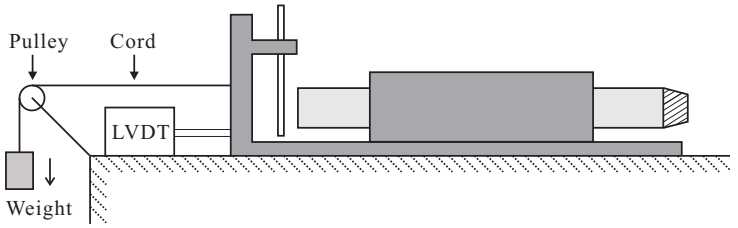

Fig. 4. Schematics of measurement of static friction coefficient

Identification of friction coefficient between the capsule and the support surface was carried out by both static and dynamic tests. The static test shown in Fig. 4 was to increase the weight slowly until the experimental rig began to move, and the static friction was calculated as the ratio of the mass of the weight to the mass of the rig. The test was run for five times, and the average value of the static coefficient was taken. The dynamic friction coefficient was calculated using the energy equivalent equation

$$\mu_d(m_1 + m_2)gd = \tfrac{1}{2}(m_1 + m_2)v^2, \tag{2}$$

where $\mu_d = \frac{v^2}{2gd}$ is the dynamic friction coefficient to be identified, d is the travel distance of the capsule, and v is the initial velocity of the capsule. The dynamic test was to give the capsule an arbitrary initial speed v by pushing it gently and measure the travel distance of the capsule d subject to dynamic friction. The dynamic test was run for six times, and the dynamic coefficients were found to be well approximated by the Coulomb Stribeck model[16] as demonstrated in Fig. 3(b). Finally, the identified physical parameters of the vibro-impact capsule system are given in Table 1.

4. Simulation and experimental results

This section compares the simulation results obtained from the proposed mathematical model with the experimental results. There were five trials for each experiment and the repetitive results are consistent. All the experimental data were smoothed by using the Savitzky-Golay algorithm so that noise from the measurement can be filtered out.

An example of experimental data obtained for $k_2 = 2.42$ kN/m, $\omega = 77.91$ rad/sec, $p_d = 4$ N, and $\delta = 3.5$ mm is presented in Fig. 5. It can be seen from Fig. 5(a) that the overall progression of the capsule is forward, but the capsule has backward motion per period of external excitation. As the support spring is relatively soft, the impact action of the rod is not obvious in Fig. 5(b). However, the impact can be identified from the signals obtained from the accelerometer mounted on the rod as shown in Fig. 5(c), where the points of impact are easily recognizable in

Table 1. Identified physical parameters of the capsule system[20]

Parameters	Value
m_1	0.11 kg
m_2	0.53 kg
k_1	1.42 kN/m
c	3.89 Ns/m
μ	0.66
ν_s	0.3
k_2	Various in kN/m
Ω	Various in Hz
P_d	Various in N
G	Various in mm

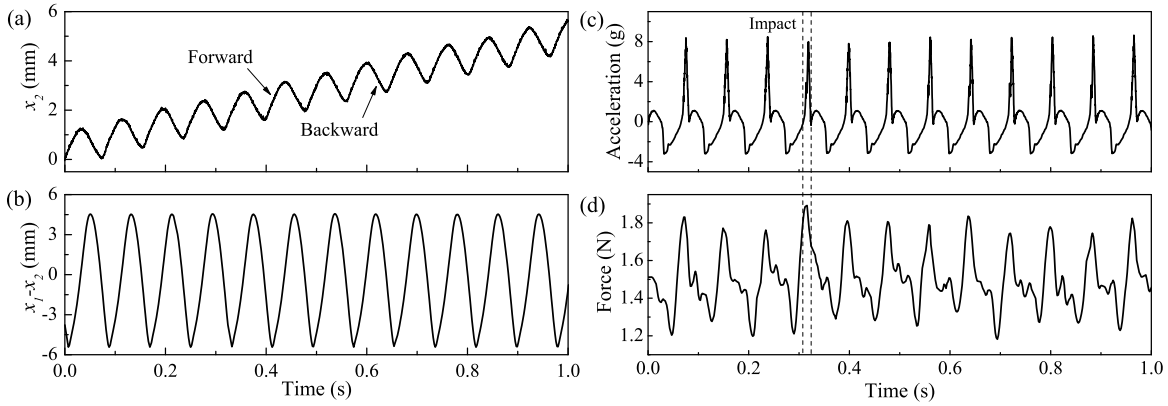

Fig. 5. Time histories of (a) the capsule displacement, x_2 and (b) the relative displacement, $x_1 - x_2$ obtained at $k_2 = 2.42$ kN/m, $\omega = 77.91$ rad/sec, $p_d = 4$ N, and $\delta = 3.5$ mm.

the form of sharp spikes[21]. In Fig. 5(d), the resistant force calculated from the current of the linear servomotor is presented.

The first scenario of comparison between the numerical simulation and the experiment for $k_2 = 18.96$ kN/m, $\omega = 20.73$ rad/sec, $p_d = 4$ N, and $\delta = 1.5$ mm is shown in Fig. 6. As can be seen from Fig. 6(a,b), the mass has a high frequency vibro-impact behaviour in simulation, but the rod has only one impact with the support spring per period of excitation in experiment. Such a discrepancy could also be observed from Fig. 6(c,d) where velocities of the mass and the capsule are presented. It can be seen from Fig. 6(c) that the high frequency vibro-impact behaviour is caused by a series of impacts between the mass and the support spring, and the capsule moves forward in a stick-slip manner. This observation could be explained as either insufficient elastic forces or overestimated friction acting on the capsule in simulation. Comparing with Fig. 6(d), the capsule has only one forward motion per period of excitation in experiment indicating that the elastic forces acting on the capsule is sufficiently large to overcome the external resistance. However, comparing the overall displacements of the capsule in Fig. 6(a,b), both of them are forward and their average speeds are similar.

The comparison of capsule displacements between the simulation and the experiment for $k_2 = 59.41$ kN/m, $p_d = 2.5$ N, and $\delta = 1.5$ mm is shown in Fig. 7(a-d). As the frequency of excitation increases, the bifurcation of the capsule system from stationary to forward progression are observed in both simulation and experiment. Again, the difference in capsule displacements are due to either insufficient elastic forces or overestimated friction acting on the capsule. In other words, the stiffness of the support spring might not be perfectly linear in experiment which contradicts with our assumption in simulation. Alternatively, the static friction used in simulation might be larger than the actual resistance in experiment. This statement could be revealed by Fig. 7(e,f) where time histories of displacements of the mass for

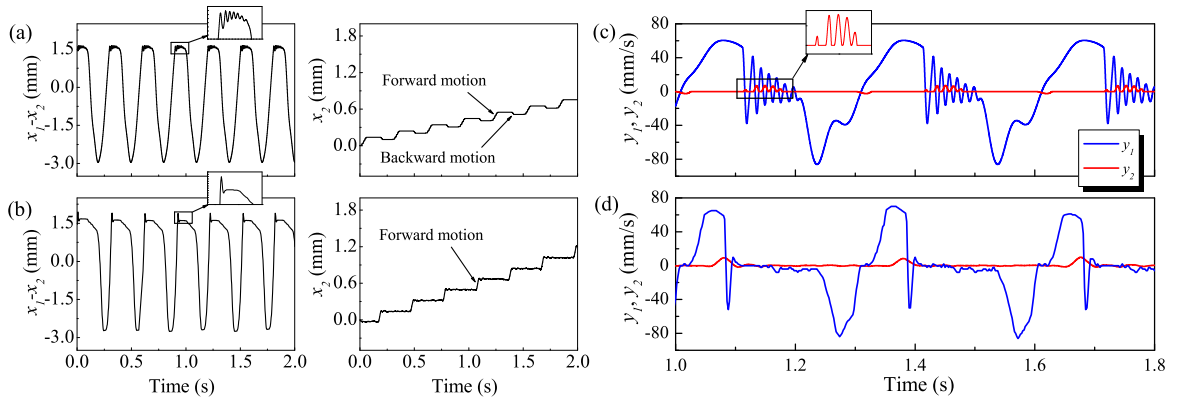

Fig. 6. Time histories of the relative displacement, x_1-x_2 and the capsule displacement, x_2 obtained (a) numerically and (b) experimentally, and time histories of velocities of the mass, y_1 (blue line) and the capsule, y_2 (red line) obtained (c) numerically and (d) experimentally at k_2 = 18.96 kN/m, ω = 20.73 rad/sec, p_d = 4 N, and δ = 1.5 mm.

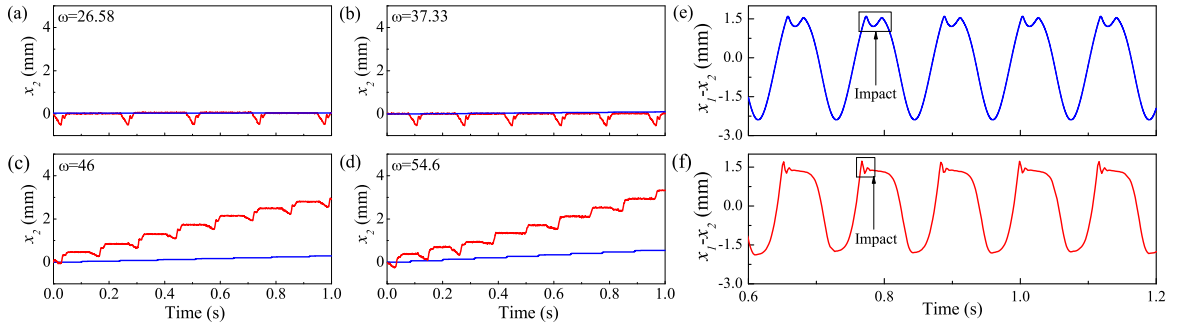

Fig. 7. Time histories of the capsule displacement, x_2 obtained numerically (blue lines) and experimentally (red lines) at (a) ω = 26.58 rad/sec, (b) ω = 37.33 rad/sec, (c) ω = 46 rad/sec, and (d) ω = 54.6 rad/sec, k_2 = 59.41 kN/m, p_d = 2.5 N, and δ = 1.5 mm. Time histories of the relative displacement, x_1-x_2 obtained (e) numerically and (f) experimentally for ω = 54.6 rad/sec.

ω = 54.6 rad/sec are presented. As can be seen from the figure, the capsule is able to undertake two impacts per period of excitation from the mass in simulation, however only one impact is observed in experiment because of the rapid forward motion of the capsule after the impact.

5. Conclusions

A modelling and experimental investigation of the vibro-impact capsule system was undertaken in this work by using a novel experimental test bed. In the considered mathematical model, the capsule system is excited by the harmonic force applied to the inner mass, and non-smooth multibody dynamics was applied to describe the motion of the system. The merit of the system is that no external driving mechanism is required so that the system can be encapsulated and move independently in the complex environment, such as engineering pipeline or gastrointestinal tract.

Numerical simulations and experimental results were compared extensively showing that the mathematical model and the experiment had a good agreement. Although some discrepancies were observed, they were within an acceptable level, and we still could conclude that the proposed mathematical model is able to predict well the main motion of the capsule system. These discrepancies could be explained as the inaccuracies in measuring the stiffness of the support spring or in identifying friction coefficients. Since the support spring is a thin steel leaf spring, our assumption in simulation is that it provides perfectly linear elastic force during the contact. Regarding to the identification of friction coefficients, it simply assumes that all the contacting points obey the Stribeck friction model in simula-

tion, whereas the resistance from practical environment is anisotropic and the base frame has a large contacting area which is asymmetric in experiment. The authors believe that the above two issues are the two main reasons causing discrepancies.

Acknowledgements

Dr. Yang Liu would like to acknowledge the financial support for the Small Research Grant (31841) by the Carnegie Trust for the Universities of Scotland. This work is also partially supported by the National Natural Science Foundation of China (Grant Nos. 11672257 and 11402224), the Natural Science Foundation of Jiangsu Province of China (Grant No. BK20161314).

References

1. Z. Wang, and H. Gu "A bristle-based pipeline robot for I11-constraint pipes," *IEEE T Robot*, vol. 13, pp. 383-392, 2008.
2. Y. Zhang, S. Jiang, X. Zhang, X. Ruan, and D. Guo "A variable-diameter capsule robot based on multiple wedge effects," *IEEE-ASME T Mech*, vol. 16, pp. 241-254, 2011.
3. J. Park, D. Hyun, W. Cho, T. Kim, and H. Yang "Normal-force control for an in-pipe robot according to the inclination of pipelines," *IEEE Trans. Industrial Electronics*, vol. 58, pp. 5304-5310, 2011.
4. P. Glass, E. Cheung, and M. Sitti, "A legged anchoring mechanism for capsule endoscopes using micropatterned adhesives," *IEEE Trans. Biomedical Engineering*, vol. 5, pp. 2759-2767, 2008.
5. M. Simi, P. Valdastri, C. Quaglia, A. Menciassi, and P. Dario, "Design, fabrication and testing of a capsule with hybrid locomotion for gastrointestinal tract exploration," *IEEE-ASME T Mech*, vol. 15, pp. 170-180, 2010.
6. S. Yim and M. Sitti, "Design and rolling locomotion of a magnetically actuated soft capsule endoscope," *IEEE T Robot*, vol. 28, pp. 183-194, 2012.
7. H. Zhou, G. Alici, T. Than, and W. Li "Modeling and experimental investigation of rotational resistance of a spiral-type robotic capsule inside a real intestine," *IEEE-ASME T Mech*, vol. 18, pp. 1555-1562, 2013.
8. M. Quirini, A. Menciassi, S. Scapellato, C. Stefanini, and P. Dario, "Design and fabrication of a motor legged capsule for the active exploration of the gastrointestinal tract," *IEEE-ASME T Mech*, vol. 13, pp. 169-179, 2008.
9. Z. Nagy, R. Leine, D. Frutiger, C. Glocker, and B. Nelson "Modeling the motion of microrobots on surfaces using nonsmooth multibody dynamics," *IEEE T Robot*, vol. 28, pp. 1058-1068, 2012.
10. R. Carta, M. Sfakiotakis, N. Pateromichelakis, J. Thoné, D. P. Tsakiris, and R. Puers "A multi-coil inductive powering system for an endoscopic capsule with vibratory actuation," *Sensors and Actuators A*, vol. 172, pp. 253-258, 2011.
11. M. Sfakiotakis, N. Pateromichelakis, and D. Tsakiris "Vibration-induced frictional reduction in miniature intracorporeal robots," *IEEE T Robot*, vol. 30, pp. 1210-1221, 2014.
12. Y. Liu, M. Wiercigroch, E. Pavlovskaia, and H. Yu "Modelling of a vibro-impact capsule system," *Int J Mechanical Sciences*, vol. 66, pp. 2-11, 2013.
13. H. Fang and J. Xu "Dynamics of a mobile system with an internal acceleration-controlled mass in a resistive medium," *J. Sound and Vibration*, vol. 330, pp. 4002-4018, 2011.
14. F. Chernousko "The optimum rectilinear motion of a two-mass system," *J. Appl. Math. Mech.*, vol. 66, pp. 1-7, 2002.
15. F. Chernousko "The optimum periodic motions of a two-mass system in a resistant medium," *J. Appl. Math. Mech.*, vol. 72, pp. 116-125, 2008.
16. Y. Liu, E. Pavlovskaia, D. Hendry, and M. Wiercigroch "Vibro-impact responses of capsule system with various friction models," *Int J Mechanical Sciences*, vol. 72, pp. 39-54, 2013.
17. H. Li, K. Furuta, and F. L. Chernousko "Motion generation of the Capsule bot using internal force and static friction," IEEE Int. Conf. on Decision and Control, pp. 6575-6580, 2006.
18. C, Zhang, H. Liu, and H. Li "Modeling of frictional resistance of a capsule robot moving in the intestine at a constant velocity," *Tribol Lett*, vol. 53, pp. 71-78, 2014.
19. Y. Liu "Experimental Study of a Vibro-Impact Capsule System," the 14^{th} IFToMM World Congress, Taipei, Taiwan, October 2015.
20. Y. Liu, E. Pavlovskaia, and M. Wiercigroch "Experimental verification of the vibro-impact capsule model," *Nonlinear Dyn*, vol. 83, pp. 1029-1041, 2015.
21. J. Ing, E. E. Pavlovskaia, M. Wiercigroch, and S. Banerjee, "Experimental Study of Impact Oscillator with One-Sided Elastic Constraint," *Philos. Trans. R. Soc. A*, vol. 366, pp. 679C704, 2008.